

# Design Methodology for Biped Robots: Applications in Robotics and Prosthetics

Máximo Roa, Diego Garzón and Ricardo Ramírez  
*National University of Colombia*  
*Colombia*

## 1. Introduction

Bipedal walk as an activity requires an excellent sensorial and movement integration to coordinate the motions of different joints, getting as a result an efficient navigation system for a changing environment. Main applications of the study of biped walking are in the field of medical technology, to diagnose gait pathologies, to take surgical decisions, to adequate prosthesis and orthosis design to supply natural deficiencies in people and for planning rehabilitation strategies for specific pathologies. The same principles can also be applied to develop biped machines; in daily situations, a biped robot would be the best configuration to interact with humans and to get through an environment difficult for navigation. If the biped robot is designed with human proportions, the robot could manage his way through spaces designed for humans, like stairs and elevators, and hopefully the interaction with the robot would be similar to interaction with a human being.

The National University of Colombia has been working on the design and control of biped robots, supported by two research groups, Biomechanics and Mobile Robots. The joint effort of the groups has produced three biped robots with successful walks, based on a single idea: if an appropriate design methodology exists, the resulting hardware must have appropriate dynamical characteristics, making easier the control of the walking movements. The design process successfully merges two lines of research in bipedal walk, passive and active walks, by using gait patterns obtained thanks to the simulation of a kneed passive walker to create the trajectory followed by the control of an active biped robot. Our actual line of research in biped robots is to use biped robots reproducing the human gait pattern as engineering tools to test the behavior of below-knee prostheses, thus producing a biped robot with heterogeneous legs that allows the evaluation of how the prosthetics influence the normal gait of the robot while it is walking as a human.

## 2. Design Methodology

Biped robot design should be based on a design methodology that produces an appropriate mechanical structure to get the desired walk. We use a design methodology that groups passive and active walk relying on dynamic models for bipedal gait (Roa et al., 2004). The methodology is an iterative process, as shown in Fig. 1. The knowledge of biped robot

Source: Climbing & Walking Robots, Towards New Applications, Book edited by Houxiang Zhang, ISBN 978-3-902613-16-5, pp.546, October 2007, Itech Education and Publishing, Vienna, Austria

dynamics allow us to develop simple and efficient control systems, based on the system dynamics and not on assumptions of a simplified model, such as the inverted pendulum, which provides valid results in simulation, but validation is difficult because of the challenge represented by the measure of position, speed or acceleration of the centre of mass in a real robotic mechanism.

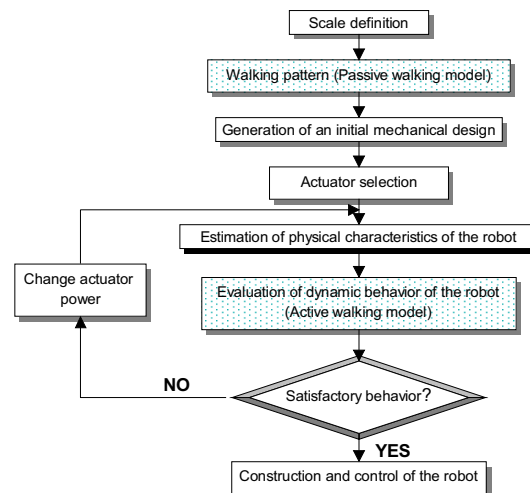


Fig. 1. Design methodology for biped robot design

The dynamical model for an actuated walk is the base in the design methodology used here; it is presented in Section 3. Geometrical and kinematical data are used to solve the model. Geometric variables of the robot (mass, inertia moment, length, and position of the centre of mass for each link) can be defined with different criteria, e.g. if the biped robot is intended to be a model of human gait, it is useful to scale anthropometrical proportions with a suitable scale factor. These data can be easily acquired using a CAD solid modeler software for a preliminary design. Kinematical data constitute the gait pattern for the robot. This pattern can be acquired from two approximations: extracted from a gait analysis of normal people in a gait laboratory, or generated through the simulation of passive walking models. The last approach has proved useful to obtain gait patterns at different speeds. The methodology outlined here assures that the controlled system is mechanically appropriate to get the desired walking patterns.

### 3. Dynamical Models for Biped Walkers

The main step in the development of a biped robot is the study and modeling of bipedal walk. The dynamical study can be accomplished from two points of view: passive and active walk. In passive walk the main factor is the gravitational influence on artificial mechanisms, getting a device to walk down a slope without actuators or control. In active walk there are different actuators which introduce energy to the mechanism so it can walk as desired. The models, passive and active, begin with a symmetry assumption: the geometric variables for the two legs are identical. Besides, the two legs are composed of rigid links connected by pin

joints, so each joint has just one degree of freedom. Although real walk is a three dimensional process, the models (and robots) will consider a planar walk, describing the movements in the sagittal plane (progression plane) of motion.

### 3.1 Passive Walk

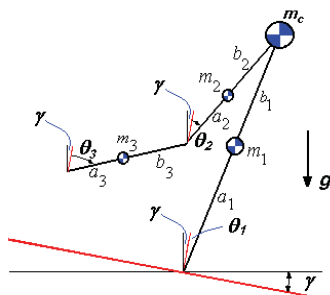


Fig. 2. Kneed-passive walker

McGeer (McGeer, 1990) presented the passive walk concept based on the hypotheses of understanding human gait as the influence of a neuromotor control mechanism acting on a device moved only by the gravity influence (Mochon & McMahon, 1980). McGeer first studied the passive walk through simple models, developed subsequently by different researchers (Goswami et al., 1996; Garcia et al., 1998). The model used in this work is the passive dynamic walker with knees (Fig. 2), original of McGeer (McGeer, 1990; Yamakita & Asano, 2001). The model has three links: stance leg (1), thigh (2) and shank (3), and four punctual masses (each link has a concentrated mass, and there is one additional mass at the hip,  $m_c$ ). The robot has punctual feet with zero mass. Each link is described with the distal ( $a$ ) and proximal ( $b$ ) lengths to the concentrated mass in the link. The angles  $\theta$  describe the angular position of the links with respect to the vertical line, and  $\gamma$  is the slope angle.

Fig. 3 shows the diagram of a gait cycle. The cycle begins with both feet on the ground. The swing leg (thigh and shank) moves freely (under gravity action) until the knee-strike, when the thigh and shank are aligned and become one single link, preventing a hyperextension in the knee. This is the beginning of the two-links phase, when the robot behaves as a compass gait walker. The gait cycle ends when the swinging leg hits the ground (heel-strike); at this point, the swing and the stance leg interchange their roles, and a new gait cycle begins.

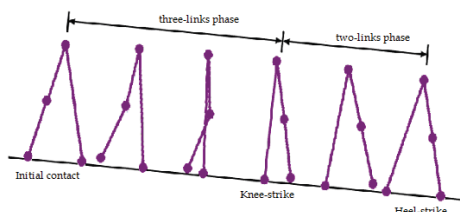


Fig. 3. Gait cycle in kneed-passive walk

Dynamic equations for the kneed-passive walker have the general matricial form

$$D(\theta)\ddot{\theta} + H(\theta, \dot{\theta})\dot{\theta} + G(\theta) = 0 \quad (1)$$

with  $D(\theta)$  the matrix of inertial terms,  $H(\theta, \dot{\theta})$  the matrix with coriolis and centripetal terms and  $G(\theta)$  the vector of gravitational effects. There are two transition events: the knee strike and the heel strike. Knee strike can be included in the above differential equation by using an artificial restriction  $\lambda_r$  (Yamakita & Asano, 2001)

$$D(\theta)\ddot{\theta} + H(\theta, \dot{\theta})\dot{\theta} + G(\theta) = -J_r^T \lambda_r \quad (2)$$

With

$$\begin{aligned} \lambda_r &= -\chi_r^{-1} J_r D(\theta)^{-1} (H(\theta, \dot{\theta})\dot{\theta} + G(\theta)) \\ \chi_r &= J_r D(\theta)^{-1} J_r^T, \quad J_r = [0 \quad -1 \quad 1] \end{aligned} \quad (3)$$

Thus, the same dynamic model can be used for the three links phase (before the knee strike) and the two links phase (after the knee strike). The transition equations for the heel strike are obtained from the conservation of angular momentum:

$$\begin{aligned} &\begin{pmatrix} m_c l_1^2 + m_1 a_1^2 + m_1 l_1 (l_1 - b_1 \cos 2\alpha) & m_1 b_1 (b_1 - l_1 \cos 2\alpha) \\ -m_1 b_1 l_1 \cos 2\alpha & m_1 b_1^2 \end{pmatrix} \begin{pmatrix} \dot{\theta}_1^+ \\ \dot{\theta}_3^+ \end{pmatrix} = \\ &\begin{pmatrix} (m_c l_1^2 + 2m_1 a_1 l_1) \cos 2\alpha - m_1 a_1 b_1 & -m_1 a_1 b_1 \\ -m_1 a_1 b_1 & 0 \end{pmatrix} \begin{pmatrix} \dot{\theta}_1^- \\ \dot{\theta}_3^- \end{pmatrix} \end{aligned} \quad (4)$$

and this event happens when  $\theta_1^- + \theta_3^- = 0$ .

To simplify the numerical simulation, we normalize the dynamic and transition equations using the following adimensional parameters

Mass ratios:

$$\mu = \frac{m_c}{m_1}, \quad \mu_1 = \frac{m_2}{m_1}, \quad \mu_2 = \frac{m_3}{m_1} \quad (5)$$

Length ratios:

$$\beta = \frac{b_1}{a_1}, \quad \beta_1 = \frac{a_2}{a_1}, \quad \beta_2 = \frac{b_2}{a_1}, \quad \beta_3 = \frac{b_3}{a_1} \quad (6)$$

However, not all of these numbers are independent; because of the symmetry of the walker there are some restrictions:

$$m_1 = m_2 + m_3, \quad l_1 = l_2 + l_3, \quad b_1 = \frac{m_2 b_2 + m_3 (l_2 + b_3)}{m_2 + m_3} \quad (7)$$

Normalized equations for the dynamical model are

$$m_1 a_1^2 \left[ D_n(\theta) \ddot{\theta} + H_n(\theta, \dot{\theta}) \dot{\theta} + \frac{1}{a_1} G_n(\theta) \right] = -J_r^T \lambda_r \quad (8)$$

With

$$D_n(\theta) = \begin{pmatrix} 1 + (\mu + \mu_1 + \mu_2)(1 + \beta)^2 & -(1 + \beta)[\mu_1 \beta_2 + \mu_2(\beta_1 + \beta_2) \cos(\theta_1 - \theta_2)] & -\mu_2 \beta_3(\beta + 1) \cos(\theta_1 - \theta_3) \\ -(1 + \beta)[\mu_1 \beta_2 + \mu_2(\beta_1 + \beta_2) \cos(\theta_1 - \theta_2)] & \mu_1 \beta_2^2 + \mu_2(1 + \beta)^2 & \mu_2 \beta_3(\beta_1 + \beta_2) \cos(\theta_2 - \theta_3) \\ -\mu_2 \beta_3(\beta + 1) \cos(\theta_1 - \theta_3) & \mu_2 \beta_3(\beta_1 + \beta_2) \cos(\theta_2 - \theta_3) & \mu_2 \beta_3^2 \end{pmatrix} \quad (9)$$

$$H_n(\theta, \dot{\theta}) = \begin{pmatrix} 0 & -(1 + \beta)(\beta_2 + \mu_2 \beta_1) \sin(\theta_1 - \theta_2) \dot{\theta}_2 & -\mu_2 \beta_3(\beta + 1) \sin(\theta_1 - \theta_3) \dot{\theta}_3 \\ -(1 + \beta) \beta_2 + \mu_2 \beta_1 \sin(\theta_1 - \theta_2) \dot{\theta}_1 & 0 & \mu_2 \beta_3(\beta_1 + \beta_2) \sin(\theta_2 - \theta_3) \dot{\theta}_3 \\ \mu_2 \beta_3(\beta + 1) \sin(\theta_1 - \theta_3) \dot{\theta}_1 & -\mu_2 \beta_3(\beta_1 + \beta_2) \sin(\theta_2 - \theta_3) \dot{\theta}_2 & 0 \end{pmatrix} \quad (10)$$

$$G_n(\theta) = \begin{pmatrix} -[1 + (\mu + \mu_1 + \mu_2)(1 + \beta)]g \sin(\theta_1 + \gamma) \\ [\mu_1 \beta_2 + \mu_2(\beta_1 + \beta_2)]g \sin(\theta_2 + \gamma) \\ \mu_2 \beta_3 g \sin(\theta_3 + \gamma) \end{pmatrix} \quad (11)$$

And the normalized heel-strike condition is

$$Q_n^+(\alpha) \theta^+ = Q_n^-(\theta) \theta^-, \text{ for } \theta^\pm = \begin{bmatrix} \theta_1^\pm \\ \theta_3^\pm \end{bmatrix} \quad (12)$$

with

$$Q_n^+(\alpha) = m_1 a_1^2 \begin{pmatrix} \mu(1 + \beta)^2 + 1 + (1 + \beta)^2 - \beta(1 + \beta) \cos 2\alpha & \beta^2 - \beta(1 + \beta) \cos 2\alpha \\ -\beta(1 + \beta) \cos 2\alpha & \beta^2 \end{pmatrix} \quad (13)$$

$$Q_n^-(\alpha) = m_1 a_1^2 \begin{pmatrix} (\mu(1 + \beta)^2 + 2(1 + \beta)) \cos 2\alpha - \beta & -\beta \\ -\beta & 0 \end{pmatrix} \quad (14)$$

The model is fully described by the set of differential nonlinear equations (8), along with the normalized heel-strike transition equations (12). The previous model is solved in Matlab using a 4<sup>th</sup> order Runge Kutta routine with numerical error of  $10^{-6}$ . In order to get a stable motion, the joint variables (displacement and velocity) must follow a cyclic trajectory. Such trajectory can be found with appropriate initial conditions at the beginning of one step. The characteristics of the gait (velocity, time period, step length) depend on the geometry and inertial properties of the robot and the slope of the plane. We arbitrarily choose ranges for the adimensional numbers and solve repeatedly the equations to find the stable limit cycle for each particular walker. Results for each particular model include the angle and velocity progression for each link vs. time (Fig. 4) and the phase planes for each of the links (Fig. 5); the example uses the same numerical values as in (Yamakita & Asano, 2001). Stability is verified through the jacobian eigenvalues, as described in (Garcia, 1999).

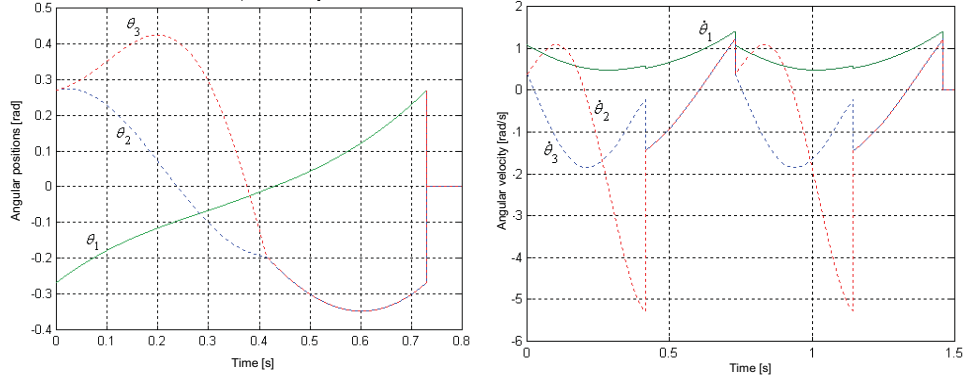


Fig. 4. Angles and angular velocity vs. time

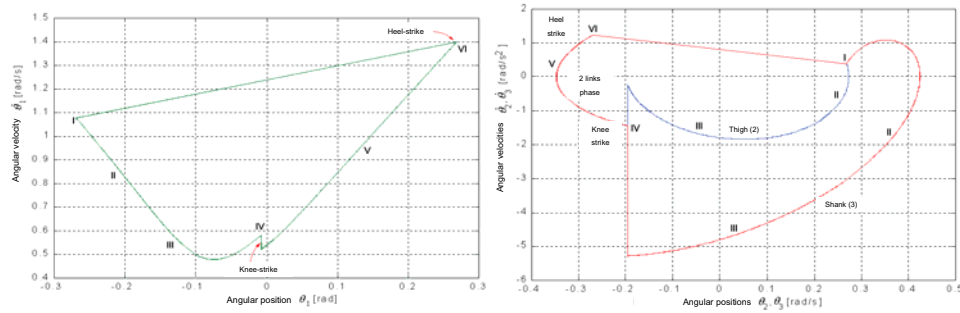


Fig. 5. Phase planes for the three links. Left: stance leg, Right: thigh and shank

The extensive simulation of the dynamical model establishes some interesting limits to get a periodic limit cycle (Roa et al., 2006). The conditions on the mass distribution (obtained with numerical simulations) to get stable limit cycles are

$$m_c > m_2 + m_3, \mu > 1, m_2 \geq m_3, \mu_1 \geq \mu_2 \quad (15)$$

And the conditions on the length ratios are

$$a_2 \geq b_2, \beta_1 \geq \beta_2, a_3 \geq b_3 \quad (16)$$

Table 1 shows the anthropometric data for mass and length in the human body (Winter, 1990). Note that the whole leg accounts for 16% of the total body mass. The human body naturally fulfills the conditions (15) and (16) provided by the numerical simulation of the passive walker, when considering the HAT mass as a concentrated mass in the hip.

Link	Link mass/Total mass of the body	Center of mass/ Link length	
		Proximal	Distal
Thigh	0.100	0.433	0.567
Shank and foot	0.061	0.606	0.394
Shank	0.0465	0.433	0.567
Complete leg	0.161	0.447	0.553
HAT (Head, Arms and Trunk)	0.678	-	-

Table 1. Mass and length for different links in the human body

Table 2 shows the relations existing between the gait parameters for two models with similar mass and length proportions in the compass gait (Goswami et al., 1996b). For instance, the walking features are identical between two models with the same mass proportion  $\mu$ . Moreover, the features for a walker with length proportion  $\beta=b_1'/a_1'$  can be compared with the features for other walker with the same ratio following the relations in Table 2, based on the scalar  $k_a=a_1/a_1'$ . As an interesting result, the same relations hold for the kneed walker. If two kneed passive robots have the same proportions (i.e. the same adimensional mass numbers) the robots have exactly the same walking behavior. Modifications in the length of link 1 keeping the same proportion with a reference model affect all the gait parameters by a scale factor, except for the angle progression vs. time. This fact gives an interesting insight into one of the supporting hypotheses in human gait analysis: that every person, no matter his height, and in consequence, his limb length (considering a normal biotype), describes the same angle trajectory for each link in his gait cycle.

Model with lengths $a_1'$ and $b_1'$	Model with lengths $a_1$ and $b_1$
$\theta$	$\theta$
$\dot{\theta}$	$\frac{1}{\sqrt{k_a}}\dot{\theta}$
$L$	$k_a L$
$T$	$\sqrt{k_a} T$
$v$	$\sqrt{k_a} v$

Table 2. Mass and length for different links in the human body

Thus, the analysis and numerical simulation of the passive walk model produces gait patterns for different slope angles in the movement of the robot (used to get different walking speeds in the real robots), which may be applied in different types of robots when considering the similarity criteria described in Table 2.

### 3.2 Actuated Walks

In dynamic walk, we consider robots moved under the effect of an actuator (servomotor, pneumatic muscle, elastic actuator, etc). The basic model used in the design process for biped robots is a five segments model, shown in Fig. 6; this model has been used previously

in other works (Lum et al., 1999). The robot has two feet, two thighs, a HAT (Head, Arms & Trunk) and punctual foot. The model of the robot has a planar walk (in the sagittal plane). Physical parameters of the model include the link mass ( $m$ ), inertia moment ( $I$ ), length ( $l$ ), distance between the center of mass and distal point of the link ( $a$ ) and the segment angle with respect to the vertical ( $\varphi$ ) (with positive direction as defined in Fig.6).

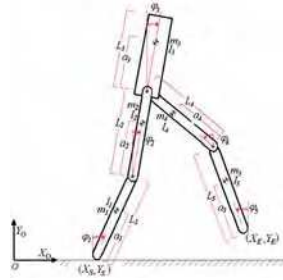


Fig. 6. Five segments model for biped walk, external torques

The gait equations, obtained with lagrangian dynamics, can be expressed in the form

$$D(\varphi)\ddot{\varphi} + H(\varphi, \dot{\varphi}) + G(\varphi) = T \quad (17)$$

with  $D(\varphi)$  a 5x5 matrix containing the inertial terms,  $H(\varphi, \dot{\varphi})$  a 5x1 vector with the effects of the coriolis and centripetal forces,  $G(\varphi)$  is a 5x1 vector containing the gravitational effects and  $T$  is the vector for moments (generalized external torques) over each segment. The components of each matrix are

Matrix of inertial terms  $D(\varphi)$

$$\begin{aligned} D_{11} &= I_1 + m_1 a_1^2 + (m_2 + m_3 + m_4 + m_5) l_1^2 \\ D_{12} &= [m_2 l_1 a_2 + (m_3 + m_4 + m_5) l_1 l_2] \cos(\varphi_1 - \varphi_2) \\ D_{13} &= m_3 l_1 a_3 \cos(\varphi_1 - \varphi_3) \\ D_{14} &= [m_4 l_1 (l_4 - a_4) + m_5 l_1 l_4] \cos(\varphi_1 + \varphi_4) \\ D_{15} &= m_5 l_1 (l_5 - a_5) \cos(\varphi_1 + \varphi_5) \\ D_{21} &= D_{12} \\ D_{22} &= I_2 + m_2 a_2^2 + (m_3 + m_4 + m_5) l_2^2 \\ D_{23} &= m_3 l_2 a_3 \cos(\varphi_2 - \varphi_3) \\ D_{24} &= [m_4 l_2 (l_4 - a_4) + m_5 l_2 l_4] \cos(\varphi_2 + \varphi_4) \\ D_{25} &= m_5 l_2 (l_5 - a_5) \cos(\varphi_2 + \varphi_5) \\ D_{31} &= D_{13} \\ D_{32} &= D_{23} \\ D_{33} &= I_3 + m_3 a_3^2 \\ D_{34} &= D_{35} = 0 \\ D_{41} &= D_{14} \end{aligned} \quad (18)$$



$$\begin{aligned}
D_{42} &= D_{24} \\
D_{43} &= D_{34} = 0 \\
D_{44} &= I_4 + m_4(l_4 - a_4)^2 + m_5 l_4^2 \\
D_{45} &= m_5 l_4(l_5 - a_5) \cos(\varphi_4 - \varphi_5) \\
D_{51} &= D_{15} \\
D_{52} &= D_{25} \\
D_{53} &= D_{35} = 0 \\
D_{54} &= D_{45} \\
D_{55} &= I_5 + m_5(l_5 - a_5)^2
\end{aligned}$$

Vector of coriolis and centripetal forces  $H(\varphi, \dot{\varphi})$ :

$$\begin{aligned}
H_1 &= [m_2 l_1 a_2 + (m_3 + m_4 + m_5) l_1 l_2] \text{sen}(\varphi_1 - \varphi_2) \dot{\varphi}_2^2 + m_3 l_1 a_3 \text{sen}(\varphi_1 - \varphi_3) \dot{\varphi}_3^2 \\
&\quad - [m_4 l_1 (l_4 - a_4) + m_5 l_1 l_4] \text{sen}(\varphi_1 + \varphi_4) \dot{\varphi}_4^2 - [m_5 l_1 (l_5 - a_5)] \text{sen}(\varphi_1 + \varphi_5) \dot{\varphi}_5^2 \\
H_2 &= -[m_2 l_1 a_2 + (m_3 + m_4 + m_5) l_1 l_2] \text{sen}(\varphi_1 - \varphi_2) \dot{\varphi}_1^2 + m_3 l_2 a_3 \text{sen}(\varphi_2 - \varphi_3) \dot{\varphi}_3^2 \\
&\quad - [m_4 l_2 (l_4 - a_4) + m_5 l_2 l_4] \text{sen}(\varphi_2 + \varphi_4) \dot{\varphi}_4^2 - [m_5 l_2 (l_5 - a_5)] \text{sen}(\varphi_2 + \varphi_5) \dot{\varphi}_5^2 \\
H_3 &= -[m_3 l_1 a_3] \text{sen}(\varphi_1 - \varphi_3) \dot{\varphi}_1^2 - [m_3 l_2 a_3] \text{sen}(\varphi_2 - \varphi_3) \dot{\varphi}_2^2 \\
H_4 &= -[m_4 l_1 (l_4 - a_4) + m_5 l_1 l_4] \text{sen}(\varphi_1 + \varphi_4) \dot{\varphi}_1^2 - [m_4 l_2 (l_4 - a_4) + m_5 l_2 l_4] \text{sen}(\varphi_2 + \varphi_4) \dot{\varphi}_2^2 \\
&\quad + [m_5 l_4 (l_5 - a_5)] \text{sen}(\varphi_4 - \varphi_5) \dot{\varphi}_5^2 \\
H_5 &= -[m_5 l_1 (l_5 - a_5)] \text{sen}(\varphi_1 + \varphi_5) \dot{\varphi}_1^2 - [m_5 l_2 (l_5 - a_5)] \text{sen}(\varphi_2 + \varphi_5) \dot{\varphi}_2^2 \\
&\quad - [m_5 l_4 (l_5 - a_5)] \text{sen}(\varphi_4 - \varphi_5) \dot{\varphi}_4^2
\end{aligned} \tag{19}$$

Vector of gravitational effects  $G(\varphi)$

$$\begin{aligned}
G_1 &= -[m_1 a_1 + (m_2 + m_3 + m_4 + m_5) l_1] g \text{sen} \varphi_1 \\
G_2 &= -[m_2 a_2 + (m_3 + m_4 + m_5) l_2] g \text{sen} \varphi_2 \\
G_3 &= -[m_3 a_3] g \text{sen} \varphi_3 \\
G_4 &= [m_4 (l_4 - a_4) + m_5 l_4] g \text{sen} \varphi_4 \\
G_5 &= [m_5 (l_5 - a_5)] g \text{sen} \varphi_5
\end{aligned} \tag{20}$$

This model contains the effect of external torques; however, torques exerted on the segments of the biped walker (human or robot) are internal moments caused by muscular forces or joint actuators; it is necessary to do an angle and torque transformation to get the internal torques in each joint. Fig. 7 illustrates the definitions for the model with internal torques. Let the vector of internal torques be

$$\tau = [\tau_1 \quad \tau_2 \quad \tau_3 \quad \tau_4]^T \tag{21}$$

with  $\tau_1$  the torque in the knee of the stance leg,  $\tau_2$  the torque in the hip of the stance leg,  $\tau_3$  the torque in the hip of the swing leg and  $\tau_4$  the torque in the knee of the swing leg. Note that four of the five degrees of freedom ( $\varphi_1, \varphi_2, \varphi_3, \varphi_4, \varphi_5$ ) may be directly controlled by the torques applied in the four joints. The angle  $\varphi_1$  in the contact point with the floor (a hypothetical joint 0) may be indirectly controlled using the gravitational effects and the

movement of the links in the robot. The existence of this underactuated DOF, that can not be directly controlled, is one of the most important features in bipedal walk.

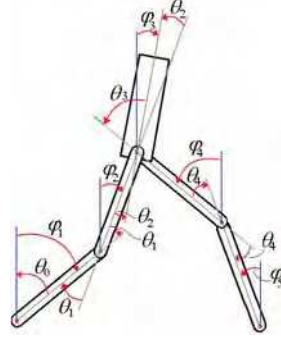


Fig. 7. Five segments model for biped walk, considering internal torques

The variables for the dynamical model with internal torques are

$$\theta = \begin{bmatrix} \theta_0 \\ \theta_1 \\ \theta_2 \\ \theta_3 \\ \theta_4 \end{bmatrix} = \begin{bmatrix} -\varphi_1 \\ \varphi_1 - \varphi_2 \\ -\varphi_2 + \varphi_3 \\ \varphi_3 + \varphi_4 \\ \varphi_4 - \varphi_5 \end{bmatrix} \quad \tau = \begin{bmatrix} \tau_0 \\ \tau_1 \\ \tau_2 \\ \tau_3 \\ \tau_4 \end{bmatrix} = \begin{bmatrix} -T_1 - T_2 - T_3 + T_4 + T_5 \\ T_2 + T_3 - T_4 - T_5 \\ -T_3 + T_4 + T_5 \\ T_4 + T_5 \\ -T_5 \end{bmatrix} \quad (22)$$

The gait equations for this model have the general form

$$d(\theta)\ddot{\theta} + h(\theta, \dot{\theta}) + g(\theta) = \tau \quad (23)$$

The components for the matrices in the previous equation are obtained directly from the dynamical model with external torques.

Matrix of inertial terms  $d(\theta)$

$$d(\theta) = [d_{i1} \quad d_{i2} \quad d_{i3} \quad d_{i4} \quad d_{i5}], \quad i=1,2,\dots,5$$

with

$$d_{i1} = -A_{i1} - A_{i2} - A_{i3} + A_{i4} + A_{i5}$$

$$d_{i2} = -A_{i2} - A_{i3} + A_{i4} + A_{i5}$$

$$d_{i3} = A_{i3} - A_{i4} - A_{i5}$$

$$d_{i4} = A_{i4} + A_{i5}$$

$$d_{i5} = -A_{i5},$$

(24)

and

$$A_{1j} = -D_{1j} - D_{2j} - D_{3j} + D_{4j} + D_{5j}$$

$$A_{2j} = D_{2j} + D_{3j} - D_{4j} - D_{5j}$$

$$A_{3j} = -D_{3j} + D_{4j} + D_{5j}$$

$$A_{4j} = D_{4j} + D_{5j}$$

$$A_{5j} = -D_{5j}$$

$$j=1,2,\dots,5$$

Vector of coriolis and centripetal forces  $H(\varphi, \dot{\varphi})$ :

$$h(\theta, \dot{\theta}) = \begin{bmatrix} h_1 \\ h_2 \\ h_3 \\ h_4 \\ h_5 \end{bmatrix} = \begin{bmatrix} -H_1 - H_2 - H_3 + H_4 + H_5 \\ H_2 + H_3 - H_4 - H_5 \\ -H_3 + H_4 + H_5 \\ H_4 + H_5 \\ -H_5 \end{bmatrix} \quad (25)$$

Vector of gravitational effects  $G(\varphi)$

$$g(\theta, \dot{\theta}) = \begin{bmatrix} g_1 \\ g_2 \\ g_3 \\ g_4 \\ g_5 \end{bmatrix} = \begin{bmatrix} -G_1 - G_2 - G_3 + G_4 + G_5 \\ G_2 + G_3 - G_4 - G_5 \\ -G_3 + G_4 + G_5 \\ G_4 + G_5 \\ -G_5 \end{bmatrix} \quad (26)$$

The initial data to solve the model are 1) geometrical data (basic dimensions of the robot) and 2) kinematical data (angular positions, velocities and accelerations in each joint). The kinematical data can be either data from a passive walk model (as the kneed passive walker) or data from a human gait analysis. Our human gait patterns were obtained in the gait laboratory at CIREC (Colombian Research Institute for Human Rehabilitation); Fig. 8 shows a gait analysis, and Fig. 9 illustrates the type of data obtained in the lab, in this case, the angular positions for each one of the joints.

The dynamical model can be simulated to get torque charts for each of the actuators composing the robot; these charts are guidelines for the appropriate actuator selection in the design process. A more complex dynamical model (for instance, a robot with seven links) may be obtained following the same guidelines previously described. Movement in the frontal plane (if required for a non-planar robot) can be modeled with the behavior of a simple inverted pendulum coupled to the movement in the sagittal plane.



Fig. 8. A gait analysis at the laboratory.

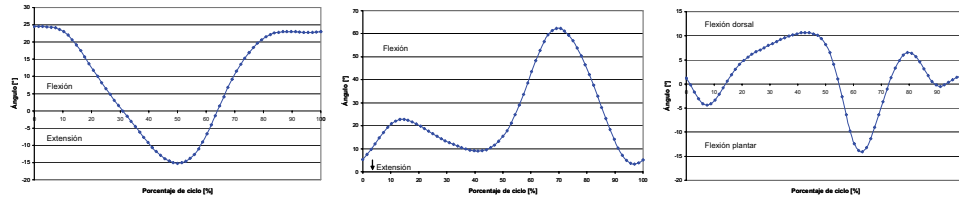


Fig. 9. Angular positions for the hip (left), knee (center) and ankle (right), as obtained from a gait analysis

## 4. Applications

### 4.1 Biped Robots

Using the proposed methodology, we have currently developed three biped robots. Our first prototype of a biped walking robot, called UNROCA-I (Fig. 10), was conceived as the simplest actuated robot that could achieve a two dimensional walk. The dynamical model for the robot has five links: a HAT and two links for each leg (the minimum required to get a walking movement in the sagittal plane, i.e. to change the supporting surface of the robot in the walking progression); it has punctual feet. The robot has two actuators in each leg (two servomotors in the knees and two at the hip). The feet are not necessary if we conceive the robot as a machine with continuous movement to keep the balance, although they are required if it is necessary to keep a static position. The robot attains a two dimensional walk thanks to a mechanical restriction, a walking guide. The robot moves with a guiding car that slides on a horizontal supporting bar. The walking guide prevents the hip oscillation in the frontal plane and the hip rotation in the transversal plane. The design preserves symmetry with respect to the sagittal plane; all of the mechanical and electrical components were mounted respecting this symmetry.



Fig. 10. Biped walking robot UNROCA-I

The robot has a trajectory following control; the position for each joint at every instant is fixed in advance (from a gait pattern), and the control system verifies this positioning. Servos have an internal feedback PD control to assure their position with a low overshoot and a fast response. Although we got a successful walking device, this prototype showed

several design and performance problems: the guide design forced us to use a counterweight to begin the walking movement, the straight line walking provides severe restrictions on the workspace, and there are differences between the predefined trajectories and the actual movements of the robot. These disadvantages forced us to completely redesign the prototype.



Fig. 11. Biped walking robot UNROCA-II

The second prototype, UNROCA-II, was conceived as a design evolution of the predecessor, thus it should solve the main problems detected in the previous one; Fig. 11 shows the prototype. Once again, we use a planar gait, but now describing a circle around a central support, getting more freedom in the robot movements; other walkers have previously used this kind of support (Pratt, 2000; Chevallereau et al., 2003). The robot uses anthropometrical proportions; it has 6 DOF, two ankles, two knees and two joints at the hips. We used normal human gait as well as passive walking gait patterns to produce the trajectory for each of the joints, so we could change the velocity of progression for the movement by changing the walking pattern; the dynamic model for the robot is the seven links model.



Fig. 12. Walking sequence for the robot UNROCA-II

We use a PD control to assure the prescribed gait: the position for each joint at every instant is given by the gait pattern, and the control system enforces this position. The internal potentiometers in the servos were used to get the reference signal for the closed loop position control. The control was implemented with microcontrollers, one for each couple of servos (for example, one micro controls the hip movements), plus a central controller to

synchronize the joint controllers. This robot corrected most of the errors of the first robot: it does not require external help to walk, and the closed loop control makes it more robust in front of perturbations. The ankle joint has two servos, making it easier to control them. The planar walk is approximated via a circular walk, eliminating the space limitations of the previous robot. The control system of the robot reacts well in the presence of small perturbations; the robot can start his walk with open (split) legs, seated or on its knees. Besides, with small obstacles in the walk path, the robot recovers its normal gait pattern once it has overcome the obstacles.



Fig. 13. Biped walking robot UNROCA-III

The third prototype of biped robot is shown in Fig. 13. This platform has picked up the previous experiences, resulting in a four DOF platform (two joints in the knees and hips), plus two passively actuated ankles. This robot does not require any external help to walk; it achieves stability thanks to an oscillating mass in top of the hip, so it actually attains a 3D walk. The oscillating mass couples and controls the gait in the sagittal and frontal planes. We used big feet to keep static stability while not moving, but they are not used to get stability in the walking process, as shown in Fig. 13; stability is assured through the appropriate movement of the counterweight in the hip according to a valid ZMP (Zero Moment Point) trajectory.



Fig. 14. Walking sequence for the robot UNROCA-III, side and front view

The three robots have achieved a satisfactory performance. From a simple point of view, the robots achieve their objective: they perform walking movements that allow them to move on two legs. The performance measurement was qualitative, as it is difficult to define parameters to measure the efficiency of movements in this kind of robots. The first robot

uses the horizontal restriction guide as an additional support. The second robot has a more satisfactory walk, although its walking style in circles implies an additional slipping effect due to the radius of the circular trajectory. The third prototype walks without any external help and without the previous problems. All of the prototypes have anthropometrical proportions and use passive walking gait patterns as well as physiological gait patterns (obtained in the gait lab at CIREC) to provide the trajectory for each one of the joints.

The fundamental achievement of these prototypes is the use of a simple control system that allows them to get a stable walk, and makes them able to overcome small perturbations. This achievement was possible thanks to the previous dynamical study, using an appropriate scaling to implement the human gait pattern and using a design methodology that takes into account the physical and dynamical features of the implemented system. Robots become an example of control systems adapting to the system dynamics, thus optimizing the power requirements on the actuators, the sensors and electronics used on the robot. The implemented gaits do not use a complex sensorial system, but the robots can extend its capabilities to become more robust to environment changes (for instance, to walk stairs).

#### 4.2 Prosthesis Evaluation

The group of Biomechanics at the National University of Colombia has developed a number of prostheses for the lower limb, such as dynamic feet, devices for alignment of total knee prostheses, and A/K & B/K (Above and below knee) prostheses; Fig. 15 shows, for instance, a damper device for lower limb prosthetics in patients with transtibial amputations (Ramirez et al., 2005). The evaluation of such devices usually implies a qualitative test using a gait laboratory to acquire data from the gait of an amputee patient; subjective criteria such as pain relief and comfort in the walk are considered as part of the evaluation. We are actually working towards the use of biped robots to avoid subjective performance evaluation of the prostheses; providing a testbed for new designs before they are tested in real patients. Other groups are developing projects along this line for A/K prostheses, in the so-called Biped Robot with Heterogeneous Legs (BRHL) (Xu et al., 2006).



Fig. 15. Damper device for lower limb prosthetics

The evaluated prosthesis replaces one of the legs of the biped robot, and the other leg is properly balanced to keep the balance of the robot. As the robot reproduces the physiological human gait pattern, the behavior of the prostheses is evaluated, thus providing reliable data on its dynamical characteristics and its influence on the global gait behavior, and avoiding the inherent subjectivity of prostheses evaluation in real patients.

## 8. References

- Chevallereau, C.; Abba, G.; Aoustin, Y.; Plestan, F.; Westervelt, E.R.; Canudas-De-Wit, C. & Grizzle, J.W. (2003). RABBIT: a Testbed for Advanced Control Theory. *IEEE Control Systems Magazine*, Vol. 23, No. 5, pp 57-79, 0272-1708.
- Garcia, M.; Chatterjee, A.; Ruina, A. & Coleman, M. (1998). The simplest walking model: stability, complexity and scaling. *ASME J. Biomechanical Engineering*. Vol.120, No.2, pp 281-288, 0148-0731.
- Goswami, A.; Benoit T. & Bernard E. (1996). *Compass – Like Biped Robot. Part I: Stability and Bifurcation of Passive Gaits*, Research Report, INRIA (Institut National de Recherche en Informatique et en Automatique), 0249-6399.
- Goswami, A.; Espiau, B. & Keramane A. (1996). Limit Cycles and their Stability in a Passive Bipedal Gait. *Proc. Int. Conf. Robotics and Automation – ICRA 1996*, pp. 246-251, 0-7803-2988-0.
- Lum, H.K.; Zribi, M. & Soh, Y.C. (1999). Planning and control of a biped robot. *Int. J. Eng. Science*, Vol.37, pp 1319-1349, 0020-7225.
- McGeer T. (1990). Passive dynamic walking. *Int. J. of Robotic Research*, Vol. 9, No.2, pp 62-82, 0278-3649.
- Mochon, S. & McMahon T. (1980). Ballistic walking: an improved model. *Mathematical Biosciences*, Vol.52, pp 241-260, 0025-5564.
- Pratt, J. (2000). Exploiting Inherent Robustness and Natural Dynamics in the Control of Bipedal Walking Robots. Ph.D. Thesis, MIT, USA.
- Ramirez, A.M.; Garzon, D.A.; Roa, M.A. & Cortes, C.J. (2005). Test on Patient of Damper Device for Lower Limb Prosthetic. *Gait & Posture*. Vol.22, No.S1, pp S48, 0966-6362.
- Roa, M.; Cortés, C. & Ramírez R. (2004). Design methodology for biped robots with an application. *Proc. CARS & FOF 2004*, pp 438-446.
- Roa, M.A.; Villegas, C.A. & Ramírez, R.E. (2006). Extensive modeling of a 3 DOF passive dynamic walker. In: *Climbing and Walking Robots*, M.O. Tokhi, G.S. Virk & M.A. Hossain, pp. 349-356, Springer, 3-540-26413-2, Berlin.
- Winter, D.A. (1979). *Biomechanics and Motor Control of Human Movement*, Wiley Interscience, 1990, 0471509086.
- Xu, X.; Xie, H.; Wang, B. & Tan, J. (2006). Gait Perception and Coordinated Control of a Novel Biped Robot with Heterogeneous Legs. *Proc. Int. Conf. Intelligent Robots and Systems – IEEE/RSJ IROS 2006*, pp. 356-361, 1-4244-0259-X.
- Yamakita, M. & Asano, F. (2001). Extended passive velocity field control with variable velocity fields for a kneed biped. *Advanced Robotics*, Vol. 115, No.2, pp 139-168, 0169-1864.





## **Climbing and Walking Robots: towards New Applications**

Edited by Houxiang Zhang

ISBN 978-3-902613-16-5

Hard cover, 546 pages

**Publisher** I-Tech Education and Publishing

**Published online** 01, October, 2007

**Published in print edition** October, 2007

With the advancement of technology, new exciting approaches enable us to render mobile robotic systems more versatile, robust and cost-efficient. Some researchers combine climbing and walking techniques with a modular approach, a reconfigurable approach, or a swarm approach to realize novel prototypes as flexible mobile robotic platforms featuring all necessary locomotion capabilities. The purpose of this book is to provide an overview of the latest wide-range achievements in climbing and walking robotic technology to researchers, scientists, and engineers throughout the world. Different aspects including control simulation, locomotion realization, methodology, and system integration are presented from the scientific and from the technical point of view. This book consists of two main parts, one dealing with walking robots, the second with climbing robots. The content is also grouped by theoretical research and applicative realization. Every chapter offers a considerable amount of interesting and useful information.

### **How to reference**

In order to correctly reference this scholarly work, feel free to copy and paste the following:

Maximo Roa, Diego Garzon and Ricardo Ramirez (2007). Design Methodology for Biped Robots: Applications in Robotics and Prosthetics, Climbing and Walking Robots: towards New Applications, Houxiang Zhang (Ed.), ISBN: 978-3-902613-16-5, InTech, Available from:  
[http://www.intechopen.com/books/climbing\\_and\\_walking\\_robots\\_towards\\_new\\_applications/design\\_methodology\\_for\\_biped\\_robots\\_applications\\_in\\_robotics\\_and\\_prosthetics](http://www.intechopen.com/books/climbing_and_walking_robots_towards_new_applications/design_methodology_for_biped_robots_applications_in_robotics_and_prosthetics)

**INTECH**  
open science | open minds

### **InTech Europe**

University Campus STeP Ri  
Slavka Krautzeka 83/A  
51000 Rijeka, Croatia  
Phone: +385 (51) 770 447  
Fax: +385 (51) 686 166  
[www.intechopen.com](http://www.intechopen.com)

### **InTech China**

Unit 405, Office Block, Hotel Equatorial Shanghai  
No.65, Yan An Road (West), Shanghai, 200040, China  
中国上海市延安西路65号上海国际贵都大饭店办公楼405单元  
Phone: +86-21-62489820  
Fax: +86-21-62489821

© 2007 The Author(s). Licensee IntechOpen. This chapter is distributed under the terms of the [Creative Commons Attribution-NonCommercial-ShareAlike-3.0 License](#), which permits use, distribution and reproduction for non-commercial purposes, provided the original is properly cited and derivative works building on this content are distributed under the same license.